

# Surface Modifications Induced by Roller Burnishing of *Ti6Al4V* Under Different Cooling/Lubrication Conditions



Giovanna Rotella and Luigino Filice

**Abstract** The paper presents a deep analysis of surface modifications induced by roller burnishing process of *Ti6Al4V* titanium alloy. The extensive experimental campaign has been performed based on a Design of Experiments at varying lubrication/cooling strategies (dry, cryogenic and MQL), roller radius, burnishing speed and burnishing depth. The resulting surface integrity has been analyzed in terms of surface roughness, micro hard-ness, microstructural changes and tribological performance. In particular, the wear rate of the burnished sample has been evaluated as a quality indicator of the process. The overall results show the influence of burnishing process parameters on surface quality and wear resistance of *Ti6Al4V* highlighting the capability of the process to significantly improve the above performance especially when cryogenic cooling is applied. Finally, the extensive experimental activity allowed to find a combination of processing parameters and lubrication conditions able to significantly improve the surface quality of the final component.

**Keywords** Burnishing · Surface integrity · Severe plastic deformation · Wear resistance

## 1 Introduction

Surface modification processes are often used to finish many components, especially those requiring high quality and service performance such as wear and corrosion

---

G. Rotella (✉)

Department of Informatics, Modeling, Electronics and Systems Engineering (DIMES), University of Calabria, 87036 Rende, CS, Italy

e-mail: [giovanna.rotella@unical.it](mailto:giovanna.rotella@unical.it)

L. Filice

Department of Mechanical, Energy and Management Engineering (DIMEG), University of Calabria, 87036 Rende, CS, Italy

e-mail: [luigino.filice@unical.it](mailto:luigino.filice@unical.it)

resistance, fatigue endurance etc. In fact, some manufacturing processes can alter the quality and geometric tolerances of the products requiring further post processing [1]. Thus, surface modification processes can be used to modify the properties of the original material limiting such changes on targeted areas of the components, typically the surface [2]. Therefore, different surface modifications can be performed according to the specific characteristics that each product needs to exhibit. Within these techniques, burnishing process is the one born to smooth the surface of machined components with interesting consequences like increase of fatigue strength and an overall enhanced surface integrity [3]. Burnishing is a cold working process in which the surface and subsurface layers' experience plastic deformation by a smooth rolling body pressed against the surface of the workpiece. The most used tools are spherical (ball burnishing) and cylindrical (roller burnishing). In the latter, the roller bodies need to be continuously in contact with the workpiece surface while rolling, thus, it is usually designed to be held and guided in a bearing system. The tool is then mounted on a milling machine or lathe and brought into contact with a machined surface with the aim to smooth the surface by applying a load greater than the yield strength of the component. Thus, the mirror like final surface and the overall superior surface integrity of the burnished product are achieved by varying a series of process parameters such as feed rate, burnishing depth, speed, roller geometry, number of passes, cooling/lubrication strategies, etc. [3–5]. Although studies have been conducted to understand the relationship within the burnishing parameters and the post processed surface integrity on many industrial materials [6–8], a clear knowledge when *Ti6Al4V* is burnished is still missing. Thus, it is crucial to perform deeper investigation aiming to assess the influence of process parameters on surface integrity of roller burnished *Ti6Al4V* and their effects on the overall wear resistance. In fact, the massive use of such alloy in the aerospace industry is mainly related to its combination of lightweight, strength, high temperature resistance and ductility. However, the poor tribological properties of titanium alloys represent still a limitation for their widespread use in many industrial fields. Thus, surface treatments of *Ti6Al4V* are commonly performed in order to improve its overall wear performance [9]. In this paper, the effects of burnishing depth, speed, cooling/lubrication techniques and tool radius on the surface integrity and wear resistance of the alloy are deeply studied by means of a full factorial Design of Experiments (DOE). The overall results offer a detailed operational framework of the burnishing processing influence on the final *Ti6Al4V* surface quality and product wear performance.

## 2 Materials and Methods

The material under investigation is the Grade 5 titanium alloy *Ti6Al4V*. The titanium bars (with a diameter of 30 mm) have been first finished by machining, subsequently, roller burnishing tests have been conducted using a high-speed CNC turning center equipped with a cooling line to supply different cooling and lubrication media. Burnishing tests have been performed using a custom-made roller-burnishing tool,

made of a hardened steel fastened to a customized crotch. The burnishing tool was connected to a piezoelectric dynamometer for force detection. The bars were mounted on a lathe with a tailstock and their length and diameter were selected to be small enough to avoid deflection of the workpiece during burnishing. The temperatures reached during the tests have been monitored by an infrared thermo-camera and the experimental campaign has been carried out under dry, minimum quantity of lubrication (MQL) and cryogenic (cryo) lubrication/cooling conditions. The MQL tests have been performed applying vegetable oil through an external nozzle to the tool-workpiece contact zone with a flow rate of 60 ml/h while the cryogenic coolant ( $\text{LN}_2$ ) has been delivered at the pressure of 6 bar through two nozzles (with an inner diameter of 2 mm) at a maximum distance to the contact region of 10 mm. It is worth pointing that the cryogenic liquid has been applied on the unprocessed surface during the process at a distance of 10 mm ahead the roller tool with a resulting pre freezing effect which avoids the problems encountered with the direct application of a conventional cryogenic process such as the risk to freeze the bearing systems holding the tool or reducing the flow capability of the material which usually lead to a poorer surface quality [4]. Figure 1 shows a schematic of the experimental equipment.

The full factorial experimental campaign has been carried out at varying burnishing speed ( $v$ ), burnishing depth ( $a_p$ ), roller radius ( $R$ ) and lubricant conditions for a total of 81 different tests with three repetitions each. The parameters used during the experimental campaign are reported in Table 1. Furthermore, an explorative preliminary experimental campaign (27 tests) has been also performed in order to select the optimal feed rate and number of passes which have been fixed to 0.05 mm/rev and 2 respectively.

The range of tested number of passes and feed rate were 1, 2 and 3 passes and 0.05, 0.1 and 0.2 mm/rev respectively according to what stated in literature [3–5]. It is worth noting that the burnishing forces have been measured as an output of the

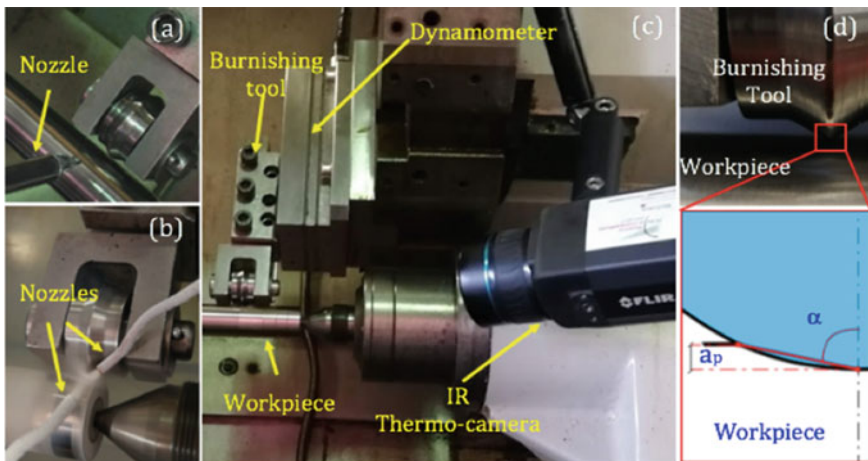


**Fig. 1** Experimental setup for **a** MQL, **b** cryogenic and **c** dry burnishing; **d** burnishing tool details

**Table 1** Design of experiments for the full factorial experimental campaign

Factor	Level 1	Level 2	Level 3
Lubricant/coolant	Dry	MQL	Cryogenic
Burnishing depth (mm)	0.1	0.3	0.5
Speed (m/min)	50	100	200
Radius (mm)	1	2.5	5

process instead of controlled input variables. This is due to the need to maintain the same burnishing depth and to guarantee the same dimensional tolerances in each of the investigated case. In fact, the proper setting of burnishing parameters is crucial to avoid exceeding the tolerance field. Moreover, it has been possible to customize the tool and the holder for the specific needs.

The cross section of burnished samples has been cut and mounted into a resin holder for further analysis. The specimens have been mechanically polished and etched using the Kroll's reagent (92 ml of distilled water, 6 ml of nitric acid, 2 ml of hydrochloric acid) and then analyzed using an optical microscope (1000×). Mean surface roughness  $Ra$  has also been measured by means of a non contact 3D confocal profilometer while the micro-hardness ( $HV_{0.01}$ ) of the surface and subsurface layer has been probed by means of an instrumented micro-nano indenter.

The microhardness tests have been carried out through the depth of the burnished samples taking into account the edge effects. Thus, in order to avoid undesired results, the first micro indentation has been performed at a distance of about 20  $\mu\text{m}$  from the burnished surface. The distance between consecutive indentations as well as that from the surface was always bigger than 3 times the longest diagonal of the impression. Another batch of burnished samples has been used to perform wear tests. In particular, a linearly reciprocating ball-on-flat sliding wear tests have been performed according to the ASTM G133 standard by means of a tribometer equipped with an alumina ball as a static partner. The tests were performed on the as received material, the burnished samples and the as machined surface.

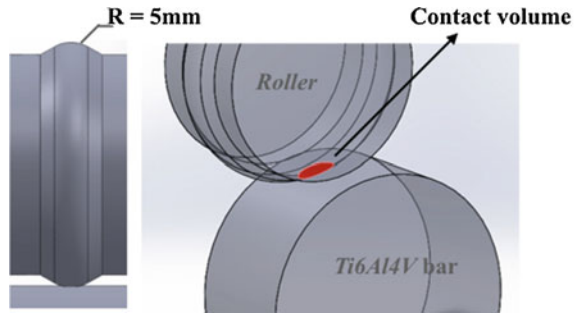
The specific wear rate, was calculated using the Archard model reported in Eq. (1)

$$W_r = V/Fn * l \text{ (mm}^3\text{/N/m)} \quad (1)$$

where  $V$  is the sample volume loss,  $F_n$  is the average normal load and  $l$  is the sliding distance. A confocal white light 3D surface profilometer was used to measure the volume loss of the burnished specimen for the evaluation of wear rate.

Figure 2 reports a further detail of the roller geometry highlighting the volume contact within the tool and the roller at a burnishing depth of 0.3 mm.

**Fig. 2** Sketch of the roller and the contact with the workpiece



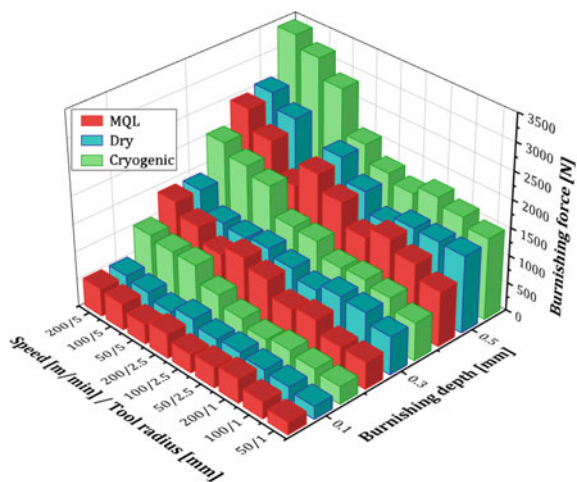
### 3 Results and Discussion

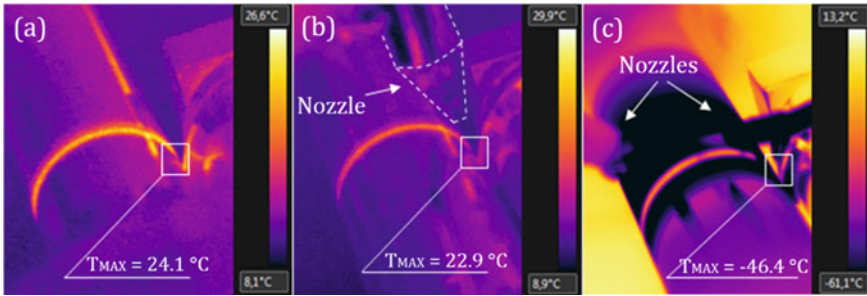
#### 3.1 Burnishing Force

Figure 3 shows as the burnishing forces, defined as the force in the radial direction, are influenced by the investigated process parameters. The burnishing forces increase with increasing of burnishing depth since a larger localized cold worked zone is created leading to higher plastic deformation.

These results are in agreement with those observed by Luo et al. [10], where it was demonstrated that burnishing forces increase approximately exponentially with the increase of the burnishing depth. Also, larger tool radius generates increasing burnishing forces even if to a lower extent than those produced by varying the burnishing depth. Moreover, the forces increase under cryogenic burnishing due to the higher strain hardening capability of the investigated alloy [11, 12]. In contrast, lower burnishing forces for dry and MQL have been measured and both conditions

**Fig. 3** Mean burnishing force measured at varying the process parameters, the tool geometry and the cooling/lubrication conditions





**Fig. 4** Steady-state measured temperatures under **a** dry, **b** MQL and **c** cryogenic conditions for a speed of 200 m/min, tool radius of 5 mm and burnishing depth of 0.5 mm

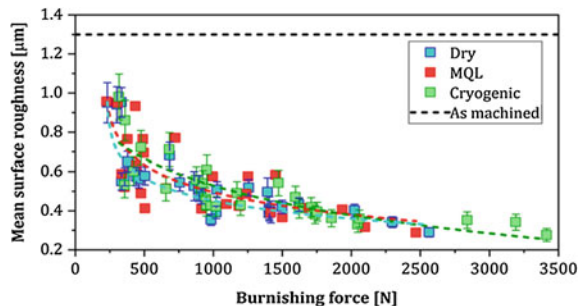
display similar trends since they work in a similar environment where little or no cooling effect is revealed (as also reported in Fig. 4).

Finally, the burnishing speed plays a little role on the variation of burnishing forces although a slight increase with increasing the speed is observed. This tendency is due to the absence of the thermal softening phenomenon since very low temperature are reached during the process (Fig. 4). Therefore, the strain rate plays a significant role on the burnishing forces variation. Thus, the low temperature variation registered during all the investigated tests also implies that no dynamic recrystallization occurs during burnishing process at the selected process conditions.

### 3.2 Mean Surface Roughness

The mean surface roughness of the as machined sample was probed to be of about  $1.32 \mu\text{m}$ . On the contrary, burnished surface roughness showed significant improvement reaching up to the 79% of reduction from the as machined surface. Figure 5 shows that with increasing of burnishing force the surface roughness decreases since surface irregularities can be reduced or eliminated by pressing the roller on the cylindrical surface.

**Fig. 5** Mean surface roughness ( $R_a$ ) of burnished samples under dry, MQL and cryogenic cooling conditions (the error bars indicate data dispersion)



This implies a greater volume of compressed material during the process which, within the investigated range of parameters, leads to a greater portion of burnished surface undergoing significant flow filling more efficiently the asperities of the machined surface and smoothing the overall sample surface. Superior burnished surface roughness can also be achieved by using larger tool radius due to geometrical and operational effects.

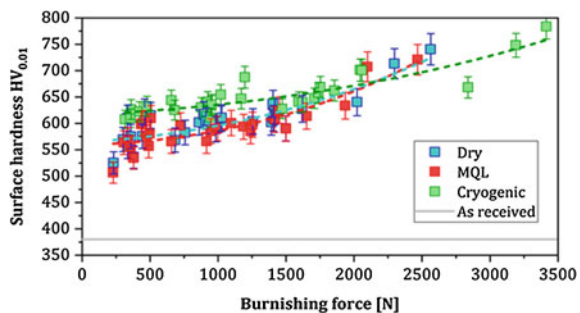
In fact, a larger radius allows to press a higher amount of material under the tool as a consequence of a higher ploughing. Also, larger radius generates higher engage angle (Fig. 1d) which determines an increase of the burnishing force and, consequently, an improvement of the surface roughness. Finally, the cooling strategy shows a slight influence on the surface roughness since for a given burnishing force the Ra values are quite similar although MQL and dry burnishing seem to create superior surface quality. These evidences can be explained by the local rise of the temperature during dry burnishing. Thus, the surface asperities can be easily deformed while, the use of LN2 condition keeps the temperature range low reducing the ability of the material to flow during the process. Finally, since the MQL condition results to a similar environment of the dry (Fig. 4), thus the Ra values are quite similar to those obtained in dry condition.

### 3.3 Microhardness and Microstructure

A significant increase of surface hardness is revealed after burnishing process as shown in Fig. 5. The results data highlight that the hardness values increase with the burnishing forces as a consequence of a greater deformation layer depths and larger localized cold worked zones. Therefore, surface hardness values increase by selecting process parameters which lead to achieve higher burnishing force (Fig. 6). Also, the difference in cooling strategy was found to have a significant impact on the surface microhardness changes.

In particular, cryogenic cooling has been proved to greatly improve the strain hardening capability during high strain severe plastic deformation [13]. Thus, for a given burnishing force, cryogenic cooling produced superior microhardness compared to

**Fig. 6** Surface hardness at varying of burnishing force and cooling strategies (as received *Ti6Al4V* has a hardness value of 380 HV; the error bars indicate data dispersion)





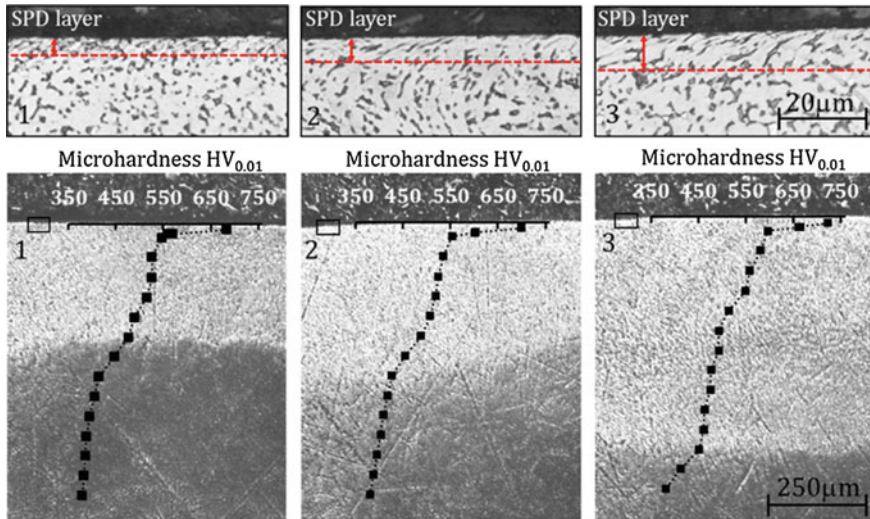


**Fig. 7** Microstructure of samples burnished under **a** MQL, **b** dry and **c** cryogenic cooling conditions and sub-surface microhardness variation

the other lubrication strategies. In contrast, MQL and dry show comparable trends since the temperatures in both conditions are quite similar as previously explained. Therefore, similar burnishing force for a fixed process condition are produced. Figure 7 shows the influence on surface integrity when samples are burnished under MQL, dry, cryogenic conditions at speed of 200 m/min, burnishing depth of 0.5 mm and a roller radius of 5 mm.

In particular, the micrographs show the formation of a deep affected layer related to the hardness changes which gradually approaches to the bulk one, together with a severe plastic deformation layer (SPD) formed in the first few microns of the affected layer. The cryogenic is the cooling methodologies that shows the more significant hardness enhancement at deeper depth, while dry and MQL burnishing show an analogous affected layers. Therefore, for a given burnishing force, the SPD and affected layers in cryogenic burnishing are larger than those experimentally observed in MQL and dry burnishing (Fig. 8).

### 3.4 Wear Resistance

Generally, wear resistance can be improved in several manners [3] and within these surface modification processes, including burnishing, are able to induce positive effects on wear properties. In particular, (Fig. 9) an increasing of wear resistance (i.e., specific wear rate is reduced) can be observed by increasing the tool radius, the speed and the depth of burnishing.



**Fig. 8** SPD layer (filled symbols) and affected layer (empty symbols) at varying of burnishing force and cooling strategies (the error bars indicate data dispersion)

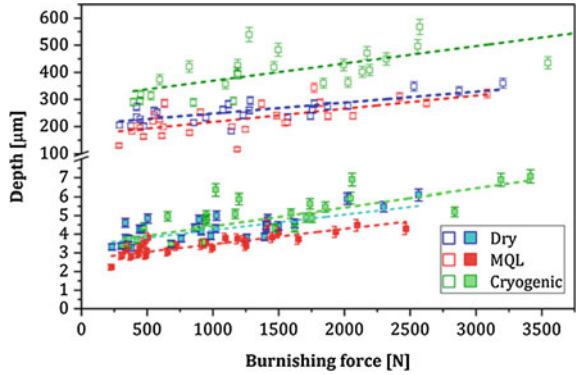
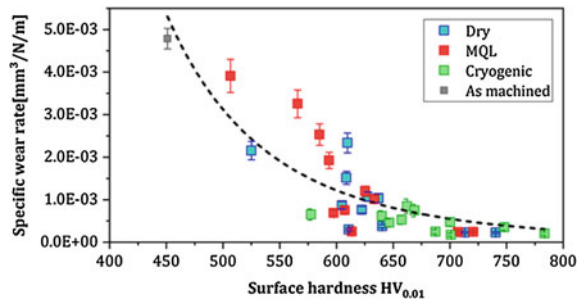


**Fig. 9** Variation of wear rate with surface hardness



The above process parameters play a synergic effect in generating higher burnishing force (Fig. 3).

Consequently, the surface hardness increases with increasing the burnishing force (Fig. 6) resulting in a lower specific wear rate. The variation of the specific wear rate as function of the surface hardness is depicted in Fig. 9.

Also the affected layer significantly influences the wear resistance since the specific wear rate is lower for larger affected layer [3]. Therefore, the cryogenic burnishing produces the superior surface in terms of wear resistance since it is able to generate deeper affected layer and higher surface hardness values.

#### 4 Overall Evaluation of Roller Burnishing of *Ti6Al4V*

The full factorial design of experiments allows to discuss the results highlighting a clear influence of the investigated process parameters and the variable of interests when burnishing *Ti6Al4V*. Figure 10 reports the main effects plot for the responses (i.e. burnishing force, mean surface roughness, affected layer, SPD layer, surface micro hardness and wear rate) versus the factors.

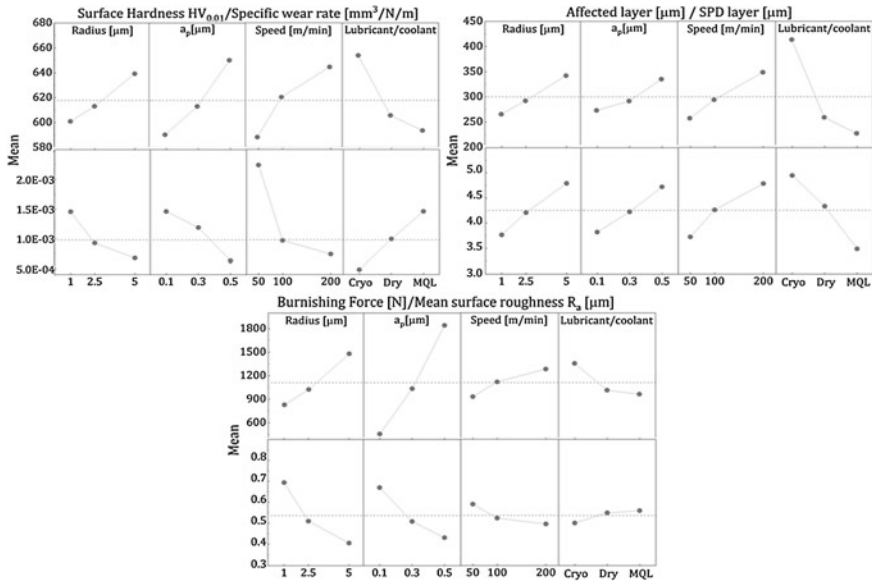


**Fig. 10** Main effects plot for the complete full factorial experimental plan

The results summarize the overall variables trends for the investigated process parameters. In particular, the beneficial effect of the cryogenic cooling condition on the surface roughness, hardness and wear rate is clearly shown in Fig. 10.

Also, the affected layer is evidently deeper when the cryogenic cooling is applied and the initial SPD layer is more pronounced. These characteristics have been demonstrated to be beneficial since they also contribute to a deeper compressive residual stresses state on the surface [3, 4]. The main effect of the speed is to increase burnishing forces, decrease surface roughness and increase the surface hardness and affected layer depth. It also shows beneficial effect in reducing the specific wear rate. The same trend is also verified for the ranges of depth of burnishing and tool radii used during the experimental campaign.

## 5 Conclusions

The extensive experimental evidences reported in this paper show the influence of burnishing process parameters on surface quality and wear resistance of Ti6Al4V. The employed process parameters were able to generate a variety of burnishing force driving the surface modifications leading, in turn, to a change in tribological performance. The experimental evidences showed a trend where higher burnishing forces increased the surface hardness, reduced roughness and improved the wear resistance. The achieved results highlight the capability of the process to significantly

improve the above performance especially when cryogenic cooling is applied. The MQL and dry also improve the wear performance of Ti6Al4V compared with the as machined one even if at a lower extent than the cryogenic one. From the other hand, when a drastic reduction of roughness is required, dry and MQL strategies offer the best results. Finally, the outcomes of this study allow to clearly find a combination of process parameters, within the investigated levels, able to offer the best surface quality according to the specific needs and applications of the Ti6Al4V components.

## References

1. Jawahir IS, Brinksmeier E, M'Saoubi R, Aspinwall DK, Outeiro JC, Meyer D, Umbrello D, Jayal AD (2011) Surface integrity in material removal processes: recent advances. *CIRP Ann Manuf Technol* 60(2):603–626
2. Rotella G, Alfano M, Candamano S (2015) Surface modification of Ti6Al4V alloy by pulsed Yb-laser irradiation for enhanced adhesive bonding. *CIRP Ann Manuf Technol* 64(1):527–530
3. Schulze V, Bleicher F, Groche P, Guo YB, Pyun YS (2016) Surface modification by machine hammer peening and burnishing. *CIRP Ann Manuf Technol* 65(2):809–832
4. Caudill J, Schoop J, Jawahir IS (2018) Correlation of surface integrity with processing parameters and advanced interface cooling/lubrication in burnishing of Ti-6Al-4V alloy. *Adv Mater Process Technol* (in press)
5. Devaraya Revankar GD, Shetty R, Rao SS, Gaitonde VN (2017) Wear resistance enhancement of titanium alloy (Ti-6Al-4V) by ball burnishing process. *J Mater Res Technol* 6(1):13–32
6. Abrao AM, Denkena B, Breidenstein B, Mörke T (2014) Surface and subsurface alterations induced by deep rolling of hardened AISI 1060 steel. *Prod Eng Res Dev* 8:551–558
7. Brinksmeier E, Garbrecht M, Meyer D (2008) Cold surface hardening. *CIRP Ann Manuf Technol* 57(1):541–544
8. El-Taweel T, El-Axir M (2009) Analysis and optimization of the ball burnishing process through the Taguchi technique. *Int J Adv Manuf Technol* 41(3–4):301–310
9. Borgioli F, Galvanetto E, Iozzelli F, Pradelli G (2005) Improvement of wear resistance of Ti-6Al-4V alloy by means of thermal oxidation. *Mater Lett* 59:2159–2162
10. Luo H, Liu J, Wang L, Zhong Q (2006) Investigation of the burnishing force during the burnishing process with a cylindrical surfaced tool. *J Eng Manuf Part B* 220:893–904
11. Wang YM, Ma E, Valiev RZ, Zhu YT (2004) Tough nanostructured metals at cryogenic temperatures. *Adv Mater* 16(4):328–331
12. Wei Q, Cheng S, Ramesh KT, Ma E (2004) Effect of nanocrystalline and ultrafine grain sizes on the strain rate sensitivity and activation volume: fcc versus bcc metals. *Mater Sci Eng* 381(1):71–79
13. Jawahir IS, Attia H, Biermann D, Dufloy J, Klocke F, Meyer D, Newman ST, Pusavec F, Putz M, Rech J, Schulze V, Umbrello D (2016) Cryogenic manufacturing processes. *CIRP Ann Manuf Technol* 65(2):713–736